

Age-dependent dynamics of neuronal VAPB^{ALS} inclusions in the adult brain

A Thesis

submitted to

Indian Institute of Science Education and Research Pune in partial fulfilment of
the requirements for the degree of MS by Dissertation

by

Pulkit



Indian Institute of Science Education and Research Pune

Dr. Homi Bhabha Road,

Pashan, Pune 411008, INDIA.

Date: 24 March, 2025

Under the guidance of

Supervisor: Dr. Girish Ratnaparkhi,


Professor, Department of Biology

From May 2024 to Mar 2025

INDIAN INSTITUTE OF SCIENCE EDUCATION AND RESEARCH PUNE

Certificate

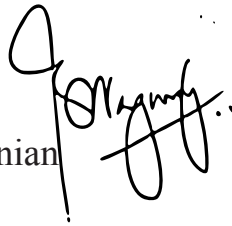
This is to certify that this dissertation entitled *Age dependent dynamics of neuronal VAPB^{ALS} inclusions in the adult brain* towards the partial fulfilment of the MS by dissertation programme at the Indian Institute of Science Education and Research, Pune represents study/work carried out by Pulkit at the Indian Institute of Science Education and Research under the supervision of Professor Girish Ratnaparkhi, Department of Biology, during the academic year 2024-2025.


Prof. Girish Ratnaparkhi

Committee:

Dr. Girish Ratnaparkhi

Dr. Nagaraj Balasubramanian



This thesis is dedicated to my family for nurturing my curiosity

Declaration

I hereby declare that the matter embodied in the report entitled *Age-dependent dynamics of neuronal VAPB^{ALS} inclusions in the adult brain* are the results of the work carried out by me at the Department of Biology, Indian Institute of Science Education and Research, Pune, under the supervision of Prof. Girish Ratnaparkhi and the same has not been submitted elsewhere for any other degree

Your Name *Pulkit*

Date: 25/03/2025

Table of Contents

| | |
|---|-----------|
| Certificate..... | 2 |
| Declaration..... | 4 |
| Table of Contents..... | 5 |
| List of Tables..... | 6 |
| List of Figures..... | 7 |
| Abstract..... | 8 |
| Acknowledgments..... | 9 |
| Contributions..... | 10 |
| Chapter 1: Introduction..... | 11 |
| Amyotrophic lateral sclerosis..... | 11 |
| A brief overview of Autophagy..... | 12 |
| An overview of VAPB and VCP..... | 13 |
| The development of the null rescue model..... | 15 |
| Change in VAPBP58S aggregate density upon autophagy and proteasomal disruption..... | 16 |
| Open questions and objectives..... | 20 |
| Chapter 2: Materials and Methods..... | 21 |
| Adult Brain dissections..... | 21 |
| Adult Brain imaging and punctae quantification..... | 21 |
| Fly husbandry and fly lines used..... | 22 |
| Negative geotaxis Motor assay for adult flies..... | 23 |
| Statistical analysis for data..... | 24 |
| Chapter 3: Results..... | 25 |
| Standardization of the aggregate staining protocol..... | 25 |
| Age dependent change in VAP positive aggregates upon Ter94 modulation..... | 26 |
| Age dependent change in aggregate density upon Atg1 modulation..... | 30 |
| Age dependent change in aggregate density upon TOR modulation in adult males..... | 32 |
| Chapter 4: Discussion and Future Perspectives..... | 34 |
| References..... | 37 |

List of Tables

| | |
|--|-----------|
| Chapter 2: Materials and Methods | 21 |
| Table 1: List of antibodies used for aggregate staining..... | 22 |
| Table 2: List of fly lines used for experiments..... | 22 |

List of Figures

| | |
|---|-----------|
| Chapter 1: Introduction..... | 11 |
| Figure 1: Schematic representation of the structure of VAP protein in Drosophila..... | 13 |
| Figure 2: Reduced lifespan and impaired motor activity in the null rescue model of VAPP58S..... | 16 |
| Figure 3: VAPP58S shows dose dependent change in aggregate density in adult fly brains..... | 17 |
| Figure 4: Atg1 knockdown causes an increase in aggregate density at day 15 in female flies..... | 18 |
| Figure 5: knockdown of Ter94 shows a decrease in aggregate density at day 15 in adult male flies..... | 19 |
| Figure 6: Overexpression of Ter94WT or Ter94R152H shows an increase in aggregate density at day 15 in adult male flies..... | 19 |
| Chapter 3: Results..... | 25 |
| Figure 7: Standardization of aggregate staining in adult fly brains..... | 25 |
| Figure 8: Effect of Ter94 modulation on VAPP58S aggregate density at day 5..... | 27 |
| Figure 9: Effect of Ter94 modulation on VAPP58S aggregate density at day 10..... | 28 |
| Figure 10: Effect of Ter94 modulation on VAPP58S aggregate density at day 15..... | 29 |
| Figure 11: Effect of Atg1 modulation on aggregate density at day 5 in adult males..... | 30 |
| Figure 12: Effect of Atg1 modulation on aggregate density on adult brains at day 10..... | 31 |
| Figure 13: Climbing assay to evaluate the change in motor ability of the flies upon Atg1 modulation..... | 32 |
| Figure 14: Change in aggregate density upon TOR modulation at day 5 in adult males..... | 33 |
| Figure 15: Change in aggregate density upon mTOR modulation at day 15 in adult males..... | 33 |

Abstract

Amyotrophic Lateral Sclerosis (ALS) is a progressive motor neuron disease that leads to motor control loss due to neuronal death. Of the ~30 genetic loci linked to familial ALS, *VAPB* (ALS8) was the 8th discovered. It encodes an ER membrane protein involved in maintaining membrane contact sites and protein trafficking. A proline-to-serine mutation at position 56 causes ALS in humans, while a similar mutation at position 58 (*VAPP58S*) is used to model ALS in flies. Mutant flies exhibit reduced lifespan, motor defects, and brain aggregates, whose density depends on mutant protein dose. Introducing a wild-type copy clears aggregates. Prior studies suggest autophagy and proteasomal system contribute to aggregate clearance, but how these pathways affect aggregate density over time remains unclear.

We investigated the role of *Atg1* and *Ter94* (homologue of VCP in flies) in aggregate dynamics in the adult fly brain at different time points. *Atg1* and *Ter94* knockdown led to increased and decreased aggregate density, respectively, aligning with previous findings. Additionally, reduced motor ability correlated with increased aggregate density in autophagy-modulated flies. However, *Ter94* modulation had minimal impact on aggregate density. This study provides a more detailed understanding of aggregate dynamics in the adult fly brain. Further exploration of interactions between *Atg1*, *VAP*, and *Ter94* could help uncover the molecular mechanisms underlying aggregate formation and clearance, offering potential insights into ALS pathology

Acknowledgments

First and foremost I would like to acknowledge Dr. Girish Ratnaparkhi for providing me the opportunity to work on this exciting project and guiding me throughout the journey of my thesis. His contributions have been instrumental in conceptualizing and supervising this work and he has been very supportive and generous throughout my time of stay.

I would also like to thank my TAC member Dr. Nagaraj Balasubramanian for his valuable insights and inputs during my thesis work. He has been of immense help to guide this project to its fruitful completion.

I would like to thank all the GR lab members for their supportive and caring nature. They have been instrumental in providing me with valuable lab skills and also helping in troubleshooting many practical problems in the lab. I thank Namrata, Lovleen, Kundan, Amrita, Sanhita, Kundan, Subhradip and Alex for their supportive company. I would also like to thank them for giving a supportive environment in the lab.

I would like to thank the fly facility and the microscopy facility at IISER Pune for providing resources to carry out the work. I would also like to thank IISER Pune for the wonderful opportunity to work there as well as for financial support.

Last but not the least, I would like to thank my friends and family for their constant support and encouragement.

Contributions

| Contributor name | Contributor role |
|------------------------------|--------------------------------------|
| Dr. Girish Ratnaparkhi | Conceptualization Ideas |
| Lovleen Garg, Sanhita Sarkar | Methodology |
| Fiji | Software |
| - | Validation |
| - | Formal analysis |
| - | Investigation |
| IISER Pune | Resources |
| - | Data Curation |
| - | Writing - original draft preparation |
| Dr. Girish Ratnaparkhi | Writing - review and editing |
| - | Visualization |
| Dr. Girish Ratnaparkhi | Supervision |
| Dr. Girish Ratnaparkhi | Project administration |
| IISER Pune | Funding acquisition |

Chapter 1: Introduction

Amyotrophic lateral sclerosis

Amyotrophic Lateral Sclerosis (ALS) is a late-onset progressive motor neuron disease. It is associated with motor neuron degeneration in the central nervous system of humans. It is a rapidly progressing disease and leads to the death of the patient in 3 to 4 years of initial symptom onset. Neuronal degradation starts in the periphery, and initial symptoms include limb weakness and tiredness. The disease then progresses to proximal motor neurons and the central nervous system causing further loss of motor control, next the patient starts to experience speech impairment, swallowing difficulty and paralysis. The patient dies of respiratory failure (*Feldman et. al., 2022*). The disease is classified into two categories: familial ALS (hereafter referred to as fALS) and sporadic ALS (hereafter referred to as sALS). 90-95% of the ALS cases are sporadic in nature with no prior history of the disease in the patient's pedigree. The remaining 5-10% patients belong to fALS and they have some genetic predisposition to the disease. There are roughly 40 genetic loci associated with ALS and some of the common loci are SOD1, FUS, TDP-43 and C9orf72. There are many rare genetic loci as well such as VAPB, VCP, CHMP2B, Alsin, etc. The exact pathophysiological mechanisms triggering the disease are not well understood but multiple cellular pathways are disrupted in ALS. These include impaired nucleocytoplasmic transport, altered RNA metabolism, impaired protein trafficking and degradation, etc. Impaired proteostasis involves disruption in the autophagy and Ubiquitin Proteasome System (UPS) (*Mejzini. et. al., 2019*).

One of the first genetic loci associated with the disease was *SuperOxide Dismutase 1 (SOD1)* in the late 1960s (*Rosen et. al., 1993*). Since then, many more genetic loci have been associated with the disease. The four common loci are SOD1, FUS, TDP43 and C9orf72. SOD1 is primarily involved in neutralizing superoxide anions to hydrogen peroxide. A glutamine to alanine mutation at 93 position in SOD1 has been associated with ALS (*Gurney et. al. 1994*). Mutant protein has been shown to block autophagy also as indicated by higher levels of p62 in mouse spinal cord extracts (*Gal et. al., 2007; Gal et. al., 2009*). FUS is another one of the four common loci which is primarily involved in juvenile ALS. FUS is an RNA Binding Protein and mutations in this gene generally disrupt its nuclear localization (*Mejzini et. al. 2019*). Similar to FUS, TAR DNA Binding Protein (TDP 43) is another protein which is usually present inside the nucleus. It has both nuclear export and nuclear localization signals and it shuttles between cytoplasm and nucleus under normal conditions. The disease models of TDP43 currently point to a disruption in the regulation of TDP-43

levels in cells which cause aberrant expression and formation of cytoplasmic aggregates (Mejzini *et. al.* 2019). Apart from these 4 loci, there are plenty of rare genetic loci associated with ALS. Some examples of those loci are VAPB, VCP, CHMP2B, etc.

A brief overview of Autophagy

Autophagy is a universal physiological pathway in eukaryotic cells which helps to clear cellular debris. It is one of the pathways disrupted in many diseases. Autophagy acts to clear both micro and macromolecular structures ranging from cellular aggregates to non-functional organelles. It is classified into three broad categories: microautophagy, macroautophagy and chaperon mediated autophagy. Macroautophagy is the most studied mechanism of autophagy. It involves the formation of a double membrane structure around the cargo to be degraded. The membrane surrounds the cargo and forms a vesicle called the early autophagosome. This autophagosome then fuses with lysosomes at late stages to form the autolysosome where the cargo is degraded by the hydrolytic enzymes present in the lysosomes (Parzych *et. al.* 2014).

The macroautophagy pathway is divided into 5 stages: Induction, elongation, closure, fusion and degradation. Induction involves the identification of the cargo meant to be degraded and initiation of the membrane formation *de novo*. Following induction, the elongation phase involves the expansion of the autophagosome membrane. The closure phase involves the completion of the autophagosome vesicle formation. The later steps of fusion and degradation involve the fusion of the autophagosome with lysosome and the degradation of the cellular cargo inside. The initiation phase in humans involves 3 proteins: ULK 1/2, Atg13 and FIP200. These 3 proteins form a stable complex in the cells. This complex is then bound to the mTORC1 complex which phosphorylates ULK1 and Atg13 thus keeping them inactive. Upon inhibition of mTORC1 complex by either rapamycin or starvation, it disassociates from the ULK1-Atg13-FIP200 complex and autophagy progresses further. During the nucleation phase, Atg14, BECN1, PIK3C3, PIK3R4 together form a complex and start the formation of the autophagosome structure. After nucleation, comes the elongation phase which involves the elongation of the membrane to enclose the cargo. At this step, LC3 or Atg8 gets lipidated in which phosphatidylethanolamine gets attached to the protein. This lipidated Atg8 is embedded in the membrane of the autophagosome. The detailed mechanisms of the later steps of the pathway are not very well known (Parzych *et. al.*, 2014).

ALS mutations in many loci have been seen to disrupt autophagy (Nguyen *et. al.*, 2019; Chua *et. al.*, 2022). One of the ALS causing loci is Ubiquilin1. It is known to associate with Atg9 and mutations in 4 of the proline residues of the protein have been shown to

disrupt this association (*Osaka et. al., 2016*). Loss of function of ubiquilin causes a significant reduction in the number of acidified lysosomes thus affecting the later stages of autophagy (*Şentürk et. al., 2019*). Another important ALS locus is TDP-43 which is a transcription factor and it shuttles between nucleus and cytoplasm using its nuclear localization and nuclear export signals (*Mejzini et. al., 2019*). Loss of TDP-43 causes a severe disruption in autophagic flux as noted by an increase in non-acidified autophagosomes (*Xia et. al., 2016*) and also a reduction in Atg7 mRNA (*Bose et. al., 2011*).

An overview of VAPB and VCP

VAPB is an Endoplasmic Reticulum (ER) membrane protein involved in protein and vesicle trafficking in the cells. It has three primary domains: Major Sperm Protein domain (MSP domain); Coiled Coiled Domain (CCD domain); Transmembrane Domain (Figure 1). It interacts with many other proteins through the presence of a conserved motif called FFAT motif in the target protein. The motif consists of two phenylalanines in an acidic tract which VAP recognizes. Humans have two forms of the protein VAPA and VAPB. A Proline to Serine mutation in the protein at 56th position (hereafter referred to as P56S) has been associated with ALS (*Nishimura et. al. 2004*).

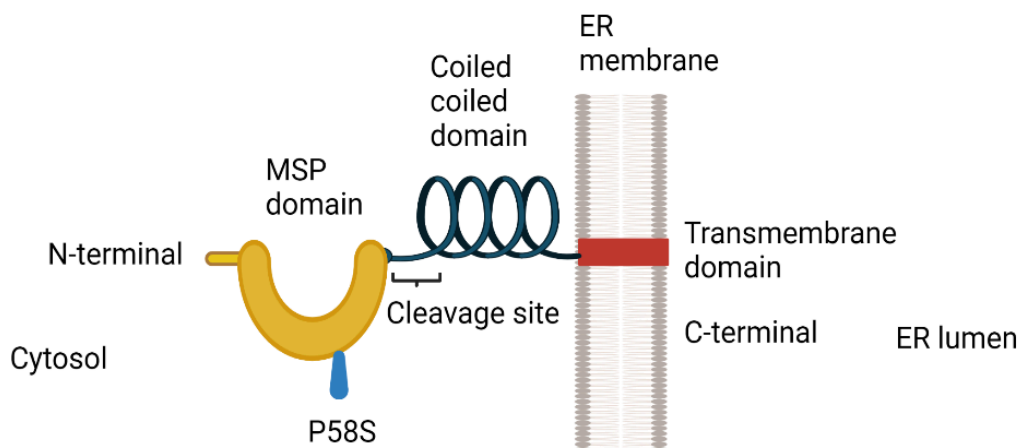


Figure 1: Schematic representation of the structure of VAP protein in *Drosophila*.

VAPB is an ER membrane protein primarily involved in protein trafficking. The protein contains Major Sperm Protein (MSP) domain, the Coiled Coiled Domain and a Transmembrane Domain. A proline to serine mutation at 58 position in the MSP domain is used to model ALS in flies. Adapted from *Lev et. al. 2008*.

VAPB has been shown to associate with proteins involved in the initial stages of autophagy. It has been shown to localize with ULK1 and FIP200 in COS7 cells. It has been shown to affect the initiation of the isolation membrane (IM) and its maturation into an autophagosome. It interacts with ULK1 and FIP200 through their FFAT motifs. The P56S mutation in VAPB which is known to cause ALS has also been shown to disrupt its interaction with ULK1 and FIP200 and it also disrupts its ability to facilitate autophagosome formation (*Zhao et. al., 2018*). In mouse models for VAP^{P56S}, the mutant protein colocalizes to autophagosomes and also causes an increase in early autophagy markers. This upregulation of autophagy seems to suggest that autophagy acts as a protective mechanism in response to the formation of VAP^{P56S} aggregates. (*Larroquette et. al., 2015*). Together these results suggest that VAP has some role to play in regulating autophagic flux and autophagy in turn acts as a protective mechanism against the VAP^{P56S} aggregates.

Valosin Containing protein (VCP) is another ALS locus. It is a homohexamer protein. It is a AAA-ATPase conserved in many organisms. The primary role of VCP is in protein clearance via the proteasomal system. The monomeric protein in mammals contains four primary domains: N terminal domain, two ATPase domains D1 and D2, and a C terminal domain. The N terminal domain is responsible for interacting with substrate protein while the D1 and D2 domains have motor activity (*Xia et. al., 2016; Chu et. al., 2023*). VCP has been identified as an ALS locus and mutation at 155th position from arginine to histidine has been shown to affect lysosomal turnover in iPSC derived motor neurons. Cells containing VCP^{R155H} mutations were not able to clear damaged lysosomes as quickly as wild type motor neurons (*Klickstein et. al., 2024*). Knockdown of VCP in mouse fibroblast cell lines disrupts the maturation of autophagosomes as noted by an increase in the levels of p62 and LC3-II positive non-acidic punctae (*Tresse et. al., 2010*). Knockdown of VCP in Inclusion Body Myopathy, Paget's Disease of bone and Frontotemporal Dementia (IBMPFD) models has also shown accumulation of autophagosomes and impairment of autophagolysosome formation (*Ju et. al. 2009*). VCP has also been shown to interact with autophagosomes at the early stages of autophagy. It has been shown to interact with Beclin 1 which is one of the early markers of autophagy and also assists in the maturation of autophagosomes (*Hill et. al. 2021*). It has also been shown that VCP interacts with ULK1 and gets phosphorylated in the process. This phosphorylation enhances the activity of VCP and aids in stress granule disassembly (*Wang et. al., 2019*). All of these results show that VCP has a major role to play in regulation of autophagy and because of the involvement of VCP in ubiquitin mediated protein clearance, it also suggests a cross talk between the proteasomal pathway and the autophagic pathway for clearance of cellular debris. The homologue for VCP in flies is Ter94

and it has a similar structure and function to VCP. *Tendulkar et al. 2022* have shown interaction between VAP and Ter94 (fly homologue of VCP) in flies through an intermediate protein called caspar (fly homologue of human faf1). Caspar protein has three primary domains: UBA domain, UAS domain and a UBX domain. The UBA domain binds to ubiquitinated proteins and the UBX domain binds to ter94. Caspar interacts with VAP through an FFAT motif present. Expression of caspar in glia has been shown to partially rescue motor defects in flies and delay the age dependent deterioration of lifespan (*Tendulkar et al., 2022*).

Drosophila melanogaster has served as an ideal model organism because of the presence of a large number of proteins which are homologous to human proteins. Human VAPs also have a homologue in flies, however, there is only a single copy of the protein present in the flies. The protein is called VAP-33. A proline to serine mutation at 58th position (hereafter referred to as VAP^{P58S}) is used to model ALS-like phenotypes in the fly.

The development of the null rescue model

Moustaqim-Barrette et al. 2013 developed a null rescue model of the VAP protein in flies. The endogenous copy of VAP on the X chromosome was modified to form a non-functional protein and a copy of the gene was introduced on the third chromosome under a genomic promoter. This model showed reduced lifespan and reduced motor activity in flies (*Moustaqim-Barrette et al. 2013*). *Tendulkar et al. 2022* later modified the Tsuda model and used a severe hypomorph of the VAP protein on the X chromosome instead of a null allele (VAP^{Δ166}). The lethality associated with the hypomorphic form of VAP was then rescued by introducing a copy of the wild type gene on the third chromosome under a genomic promoter. Both VAP^{WT} and VAP^{P58S} were introduced on the third chromosome resulting in two different lines. The VAP^{P58S} line (disease model) showed impaired motor activity and reduced lifespan similar to the Tsuda model (*Tendulkar et al. PhD Thesis 2022*). The median lifespan of the VAP^{P58S} flies is around 27 days which further gets reduced to 21 days in the presence of two copies of the mutant protein. Introduction of a VAP^{WT} copy in the background of VAP^{P58S} rescues the lifespan to 57 days which is comparable to the control genotype. The mutant flies also show age dependent decline in motor activity as assessed by the negative geotropic motor assay. Flies start to show reduced climbing between day 5 and day 10 and it progressively gets worse by day 20 as compared to control flies (Figure 2). The mutant protein also forms aggregates in the brain. (*Tendulkar et al. PhD Thesis 2022*).

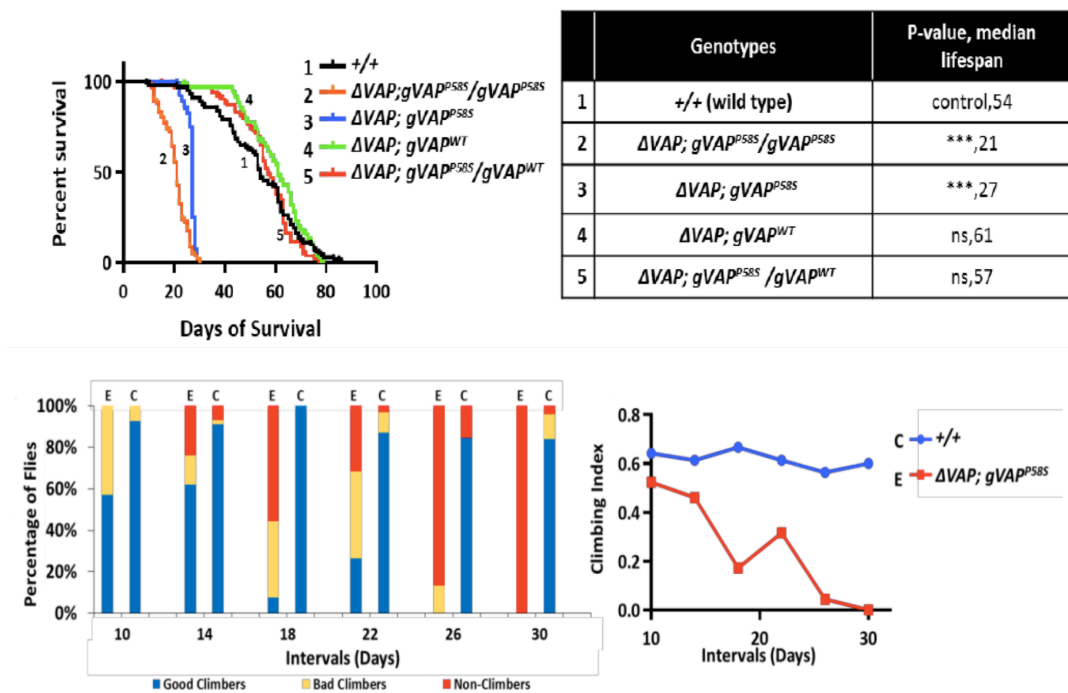


Figure 2: Reduced lifespan and impaired motor activity in the null rescue model of VAP^{P58S}.

The null rescue model was generated by deleting the VAP locus on the X chromosome and inserting a copy of VAP on the third chromosome under a genomic promoter of VAP. The top panel shows that the mutant flies have a shortened life span as compared to the control group and the introduction of a wild type copy of VAP is able to rescue the lifespan comparable to the control group. The table lists the median lifespan for each genotype and the associated p values. The bottom panel shows the proportion of non-climbers, poor climbers and good climbers as the flies age and also the deterioration in the motor activity of flies as they age. Adapted from *Tendulkar, S PhD Thesis (2022)*

Change in VAPB^{P58S} aggregate density upon autophagy and proteasomal disruption

Thulasidharan et. al. 2024, have shown the prevalence of VAPB positive aggregates in adult fly brains. These aggregates are present in the brains as early as 5 days after eclosion. The aggregate density does not seem to change as the fly ages but it is dependent on the dose of the mutant protein present. Further, the presence of a wild type copy of VAPB is able to rescue the increased aggregate density in an age dependent manner (Figure 3) (*Thulasidharan et. al. 2024*). They also explored the role of autophagy and proteasomal clearance pathways in clearance of VAP^{P58S} aggregates. To study the role of autophagy, Atg1 was knocked down in adult females using Elav-Gal4. Elav-Gal4 is a pan-neuronal gal4 expressed in all the neurons of the adult brain. The females contain a mutant copy of VAP on the third chromosome and a wild type copy of the wild type protein on the X chromosome. Upon Atg1

knockdown, there was an increase in the number of VAP^{P58S} punctae in the adult brain of females 15 days after eclosion (Figure 4).

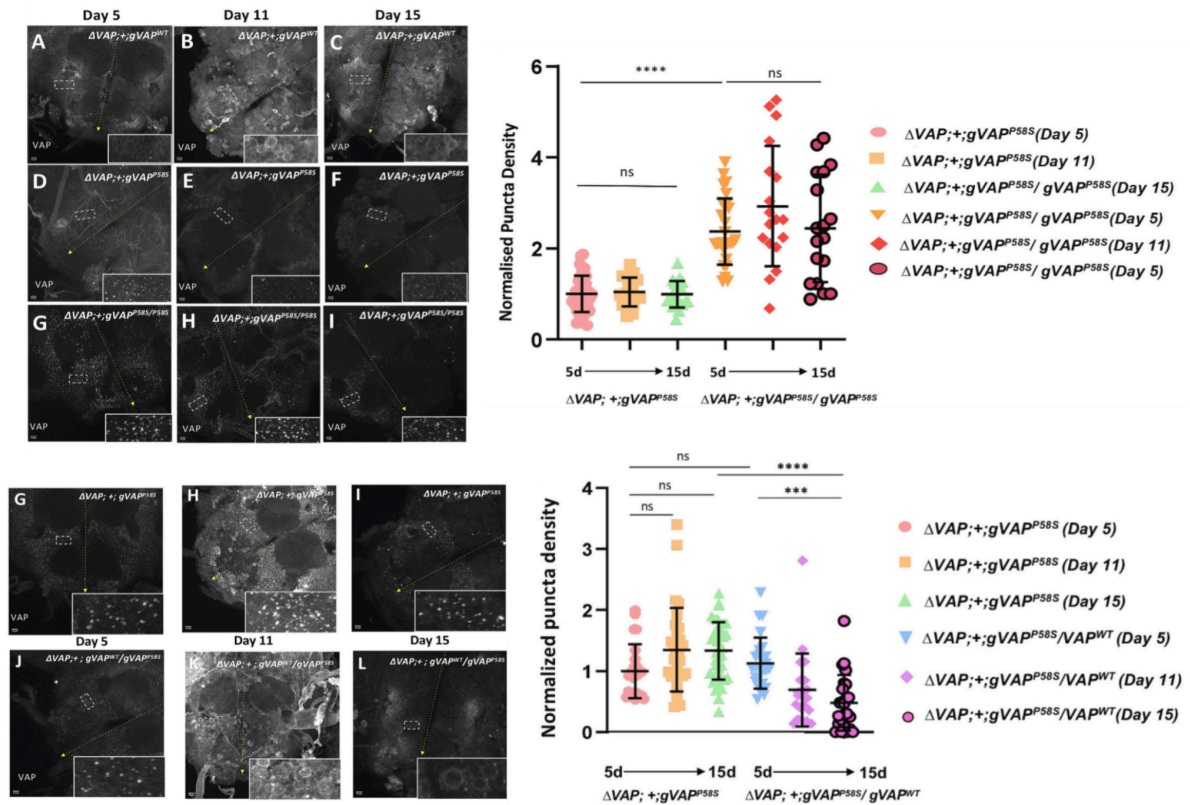


Figure 3: VAP^{P58S} shows dose dependent change in aggregate density in adult fly brains.

VAP^{P58S} is seen to form aggregates in the adult brain. The aggregate density does not change as the fly ages, however if two copies of the mutant protein are introduced, the aggregate density increases significantly. Introduction of a wild type copy of VAP in the system is able to reduce the aggregate density in an age dependent manner. Scale bars at 20 μ m. y axis represents the aggregate density normalized to the mean of the control group. *** p value < 0.001; **** p value < 0.0001. Adapted from *Thulasidharan et. al. 2024*.

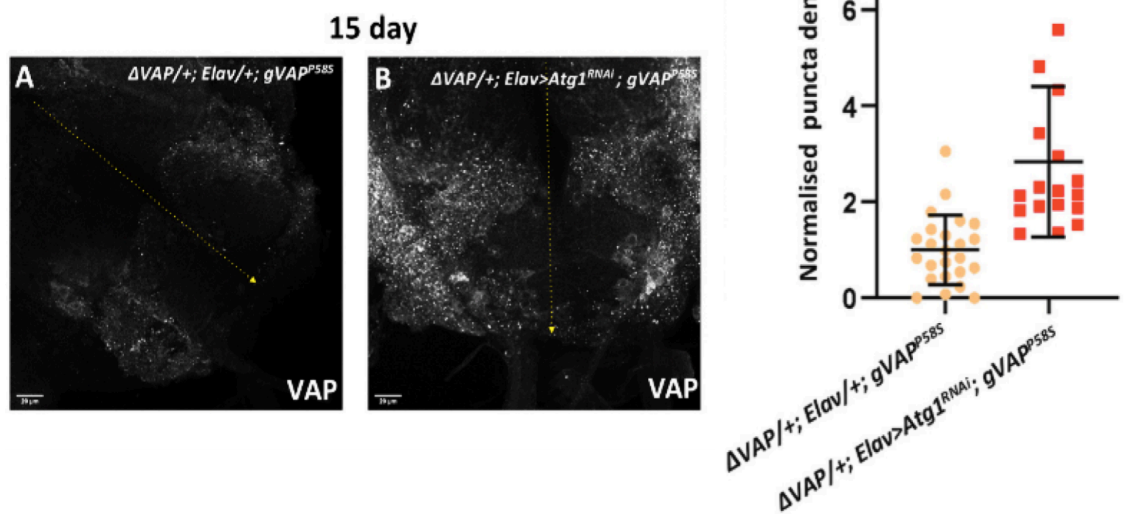


Figure 4: Atg1 knockdown causes an increase in aggregate density at day 15 in female flies.

Atg1 is one of the early initiators of autophagy in the cell and its knockdown is used to inhibit the initiation of autophagy. The aggregate density is increased compared to the respective control at day 15 in females despite having a wild type copy of VAPB. y axis represents the aggregate density normalized to the mean of the control group. ****: p value < 0.0001; scale bars at 20 μ m. Adapted from *Thulasidharan et. al. 2024*.

They have also shown that Ter94 is playing some role in stabilizing the aggregates in the adult brain. Knockdown of *Ter94* in adult brains causes a reduction in aggregate density (Figure 5) while its overexpression or expression of its dominant active mutant *Ter94*^{R152H} causes an increase in aggregate density (Figure 6). This result suggests that Ter94 is playing some role in keeping the aggregates stable despite it being an important part of the proteasomal pathway.

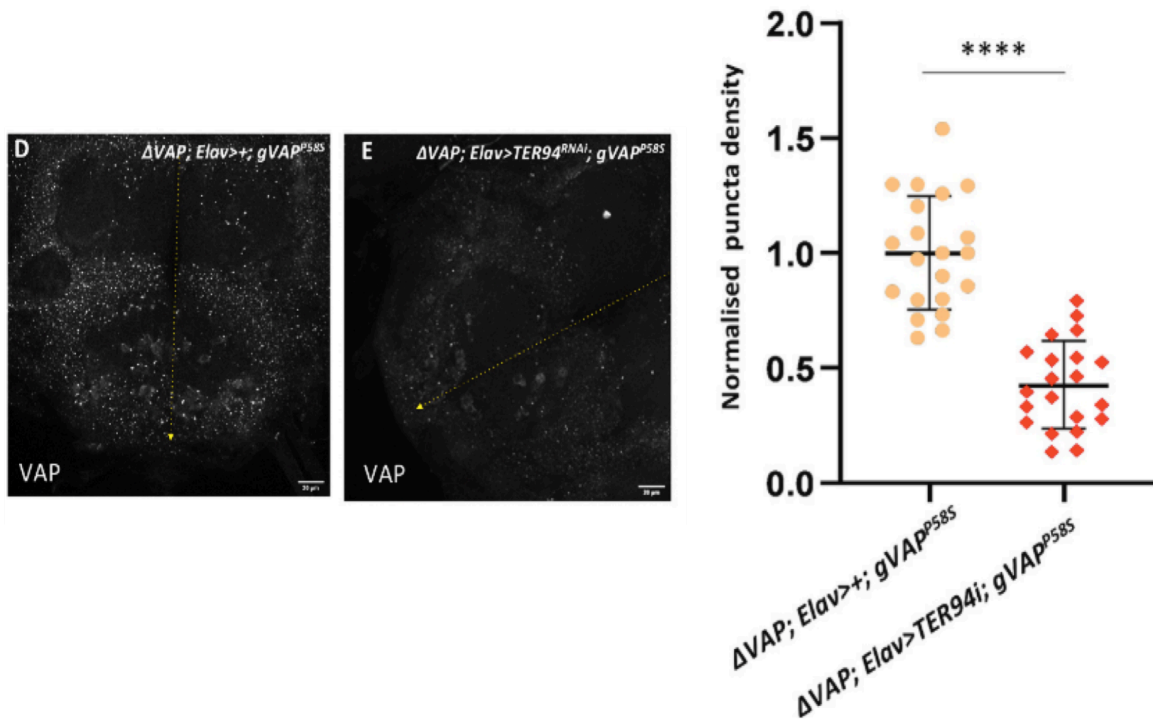


Figure 5: knockdown of *Ter94* shows a decrease in aggregate density at day 15 in adult male flies. *Ter94* is a homologue of VCP in flies and it is primarily involved in proteasomal clearance of proteins. When the protein is knocked down, the aggregate density reduces significantly at day 15 in adult males. y axis represents aggregate density normalized to the mean of the control group. **** p value < 0.0001; Scale bars at 20 μ m. Adapted from *Thulasidharan et. al. 2024*.

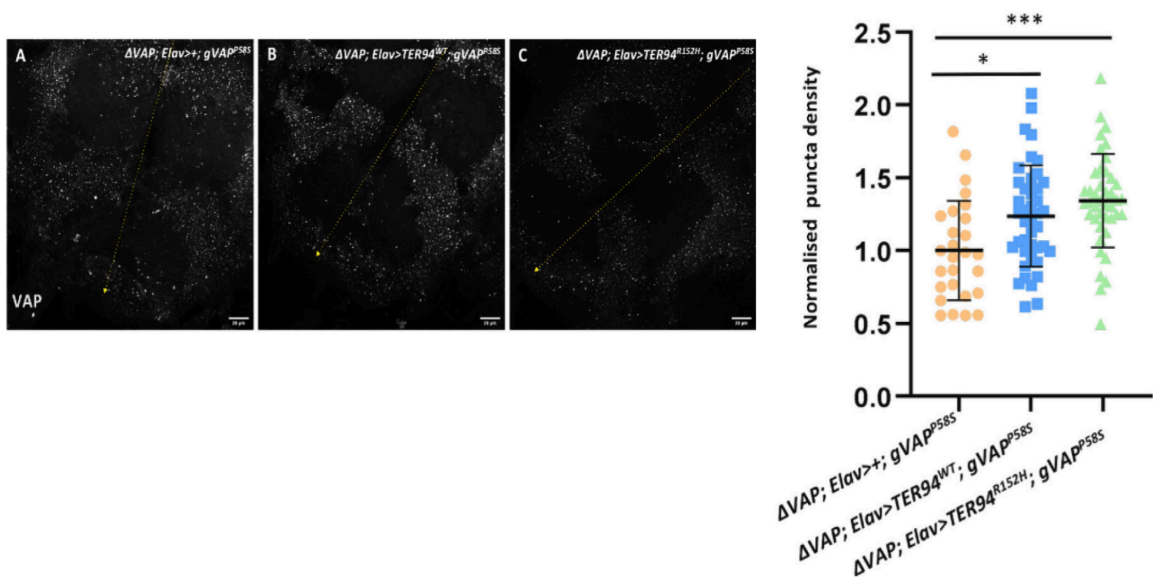


Figure 6: Overexpression of *Ter94*^{WT} or *Ter94*^{R152H} shows an increase in aggregate density at day 15 in adult male flies. Overexpression of *Ter94* causes a significant increase in aggregate density in adult male flies at day 15. The overexpression of the dominant active form of the protein *Ter94*^{R152H} also shows a significant increase in aggregate density. . * p value < 0.05; *** p value < 0.001; Scale bars at 20 μ m. Adapted from *Thulasidharan et. al. 2024*.

Open questions and objectives

The work done by *Thulasidharan et. al. 2024* suggests the role of autophagy and proteasomal machinery in maintaining the aggregate dynamics in the adult fly brain. However in the larval brain, SOD1 and therefore the Reactive Oxygen Species mediated clearance is more prevalent. Their work shows a snapshot of the state of aggregates at day 15, It is not clear how the aggregate dynamics change throughout the age of the fly. Furthermore, the role of Atg1 modulation on aggregates is studied in females which already possess a VAP^{WT} copy on the X chromosome. The relationship between Atg1 and VAP^{P58S} is not clear through the current experiments. It would be interesting to study the role of Atg1 modulation on aggregate dynamics in adult male flies at some earlier time points to get a more detailed understanding of the aggregate dynamics throughout the adult life of the mutant fly. Also elimination of the VAP^{WT} from the system would help to probe the effect of Atg1 modulation in the absence of a wild type copy of VAP. ALS is a progressive neurological disease in which the patients gradually lose motor control. If VAP^{P58S} protein aggregates are indeed playing a role in the progression of the disease, it would be interesting to see the aggregate dynamics change as the mutant fly model ages and progresses through its lifespan.

My work would primarily focus on studying the changes in VAP^{P58S} aggregates by modulating *Atg1* and *Ter94*. I would also like to study the role of the TOR pathway in affecting the aggregate density through autophagy. With these insights, we would get a better understanding of aggregate dynamics in adult fly brains and also provide crucial insights into the role of cellular clearance pathways in maintaining cellular homeostasis in disease conditions.

Chapter 2: Materials and Methods

Adult Brain dissections

The flies were anesthetized using carbon dioxide and their brains were dissected in ice cold 1X PBS. The samples were then fixed in 4% paraformaldehyde along with 0.5% triton X in 1X PBS for 1 hour at room temperature. After fixation, two simultaneous washes of 1X PBS were given and then another wash of 1X PBS was given for 15 minutes at room temperature. After that, 3 washes of 2% Bovine Serum Albumin (BSA) along with 0.3% triton X were given for 20 minutes each at room temperature. The primary antibody solution was prepared in the BSA solution with 0.3% triton X with appropriate dilution and after the washes, the samples were incubated overnight in the primary antibody solution at 4 °C . After primary incubation, the antibody solution was removed and 3 more washes of BSA with 0.3% triton X solution were given for 20 minutes each at room temperature. The samples were then incubated overnight at 4 °C in the secondary antibody solution made in the BSA with 0.3% triton X solution with appropriate dilution. After the secondary incubation, 3 more washes of BSA solutions were given and in the second BSA wash, we added Hoescht at 1:1000 dilution. After the 3 BSA washes, we removed the BSA medium and added 1X PBS. After staining, the samples were mounted on slides such that the dorsal side of the brain was facing the coverslip and invitrogen's gold antifade was used as a mounting medium.

Adult Brain imaging and punctae quantification

We used the Leica TCS SP8 confocal microscope system to image the brain samples for all of our experiments. All the brains were imaged at 63x resolution with a scan speed of 400 in 1024x1024 resolution unless otherwise noted. The bit depth was kept at 16 and z-step size was kept at 1 µm. Settings such as laser power and gain were kept constant for each independent sample in an experiment.

All the image analysis was done using ImageJ. The aggregate quantification was done using 3D Object Counter with manual thresholding. The voxel size was kept between 10 to 200 voxels. To calculate the aggregate density, 5 ROIs were selected in each brain sample between the sub-esophageal lobe and the antennae lobes and the aggregates were counted and noted for each of the ROI. The number of aggregates were then normalized against the volume of the ROI across the measured stack depth. The volume was calculated using the volume calculator plugin for ImageJ.

Table 1: List of antibodies used for aggregate staining

| Sr No. | Name of the antibody | Company/ in house | Dilution |
|--------|----------------------|--|----------|
| 1. | Rabbit anti -VAPB | In house (<i>Chaplot et. al. 2019</i>) | 1:1000 |

Fly husbandry and fly lines used

All the fly lines were maintained at room temperature. Corn meal agar was used as fly food with 6% yeast concentration. The concentration of cornmeal agar is as per Bloomington Drosophila Stock Center (BDSC) guidelines. *w¹¹¹⁸* flies were used as control and all the experiments were done using a pan-neuronal Gal4 called Elav-Gal4. A null rescue VAP^{P58S} mutant line was used to model the VAPB^{P56S} mutation in humans. The following table lists the fly lines used for experiments.

Table 2: List of fly lines used for experiments

| Sr. No | Fly line | Full genotype | Details |
|--------|-------------------------------------|---|---|
| 1. | <i>w¹¹¹⁸</i> | ++;+ | wild type control |
| 2. | $\Delta VAP; Elav-Gal4; VAP^{P58S}$ | $\Delta VAP; Elav-Gal4/CyO; VAP^{P58S}$ | null rescue system with pan-neuronal Elav Gal4. |
| 3 | ++; <i>UAS-Atg1</i> ;+ | ++; <i>UAS-Atg1/CyO</i> ;+ | Atg1 overexpression |
| 4 | ++; <i>UAS-Atg1 RNAi</i> ;+ | ++; <i>UAS-Atg1 RNAi/CyO</i> ;+ | Atg1 knockdown |
| 5 | ++;; <i>UAS-Ter94 RNAi</i> | ++;; <i>UAS-Ter94 RNAi</i> | Ter94 knockdown |

| | | | |
|---|---------------------------------------|---|---|
| 6 | <i>+,;UAS-Ter94^{WT};+</i> | <i>+,;UAS-Ter94^{WT}/CyO;+</i> | Overexpression of wild type Ter94 |
| 7 | <i>+,;UAS-Ter94^{R152H};+</i> | <i>+,;UAS-Ter94^{R152H}/CyO;+</i> | Overexpression of Ter94 ^{R152H} mutant |
| 8 | <i>+,;UAS-Ter94^{A229E};+</i> | <i>+,;UAS-Ter94^{A229E}/CyO;+</i> | Overexpression of Ter94 ^{A229E} mutant |
| 9 | <i>+,;+,;UAS-Tsc1 RNAi</i> | <i>+,;+,;UAS-Tsc1 RNAi</i> | Knockdown of Tsc1 |

Negative geotaxis Motor assay for adult flies

We also conducted an assay to check the motor abilities of flies and how it is affected by VAP^{P58S} and modulation of different genes. We used a 250 ml graduated cylinder from Borosil. The cylinder was divided into three classes: Non climbing, Poor Climbing and Climbing. The flies that were sitting on the floor of the cylinder at the end of the assay were designated as non-climbers. The flies that were able to climb to the walls but stay below the 80ml mark on the cylinder were designated as poor climbers. The flies that were able to climb up from the 80ml mark in the cylinder were designated as good climbers.

The flies were put in the cylinder and they were acclimated to the cylinder for 40 seconds. The cylinder was then tapped such that all the flies were at the bottom of the cylinder. The cylinder was then rested and the flies were then allowed to climb up the cylinder for 40 seconds. After 40 seconds, the readings were recorded for each of the 3 categories and the process was repeated 3 times with 40 second rest periods in between the readings. After the assay was completed, the flies were anesthetised by CO₂ and placed in vials. The motor assay was performed every 5 days from the date of eclosion. The exposure to CO₂ was kept minimal to prevent it from interfering with the motor ability of the flies.

The data for the motor assay was replicated 3 times for each genotype and at least 30 flies were initially taken for each biological replicate. All 30 flies were age matched. The data collected was used to calculate the climbing index of the flies. Each class of climbers is given a score and the sum of the score is then divided by the total number of flies used for the reading. The formula for calculating climbing index is given below:

$$\text{Climbing score} = 0 * NC + 3 * PC + 5 * GC$$

$$\text{Climbing Index} = \frac{\text{Climbing Score}}{\text{Total Number of flies}}$$

Where

NC = No. of non climbing flies

PC = No. of poor climbing flies

GC = No. of good climbing flies

Statistical analysis for data**Aggregate quantification**

All the aggregate data was analysed using graph pad prism 8. The data points were analysed using one way ANalysis Of Variance (ANOVA) and Bonferroni test was used as a post hoc test to correct for the occurrence of false positives that might have occurred because of manual thresholding. A minimum of 5 ROIs per brain were measured and at least 3 brains were analysed before any statistical analysis was performed.

Motor assay data analysis

The motor assay data was analysed using graph pad prism 8 software. The data points were analysed using two way ANOVA with Dunnett's multiple comparison test. A minimum of 30 statistical replicates and 3 biological replicates were used for the statistical analysis.

Chapter 3: Results

Standardization of the aggregate staining protocol

Thulasidharan et. al. 2024 have done immunostaining of VAPB aggregates using the in house rabbit anti-VAPB antibody. Although the staining protocol works well for staining VAPB positive punctae in both larval and adult brains, the long duration of the protocol was a major bottleneck. I started by standardizing a shorter staining protocol in the lab. The new staining protocol worked well for staining VAPB aggregates in the adult brain and is also shorter than the previous protocol by 2 days.

Upon staining we were able to see clear punctae of VAPB positive aggregates. The aggregates were visualized on the dorsal surface of the brain between the subesophageal lobes and the antenna lobes (Figure 7).

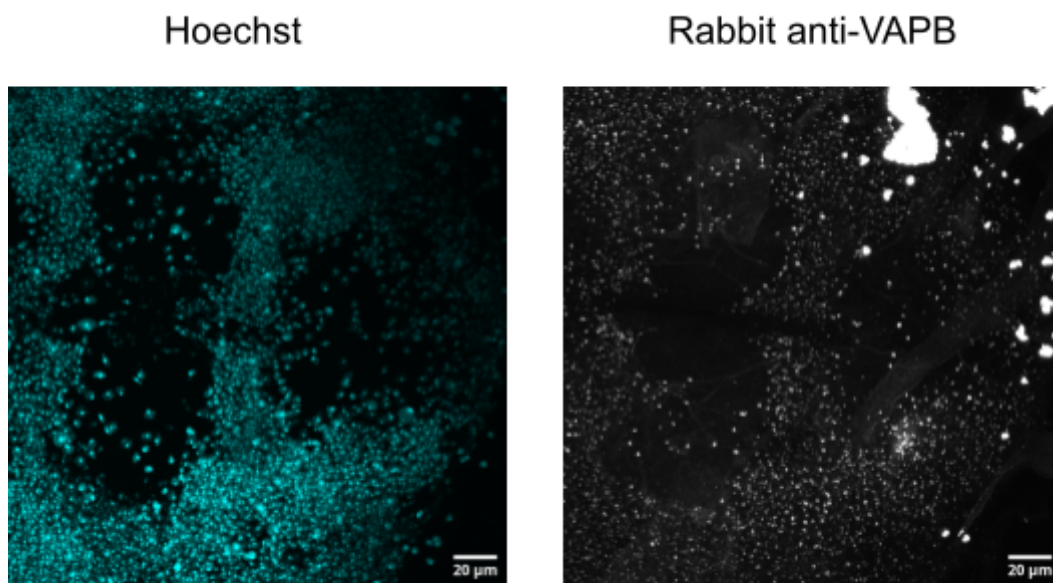


Figure 7: Standardization of aggregate staining in adult fly brains.

VAP^{P58S} forms stable aggregates in both the adult and larval brain. The aggregates were stained with rabbit anti-VAPB which was generated in the lab (*Chaplot et. al. 2019*) at 1:1000 dilution in the adult brains of 5 day old flies. Scale bar: 20 µm.. The images represent maximum intensity projections.

Age dependent change in VAP positive aggregates upon *Ter94* modulation

Thulasidharan et. al. 2024 have shown that knockdown of *Ter94* causes a decrease in aggregate density in adult brains at day 15. They have also shown that overexpression of *Ter94*^{WT} or overexpression of *Ter94*^{R152H} causes an increase in aggregates. These results suggest that *Ter94* is playing some role in stabilizing aggregates in the adult brains. Despite *Ter94* being a part of the proteasomal system, its role in stabilization of aggregates is counter intuitive. It is also not apparent that upon *Ter94* modulation, how does aggregate density change as the fly ages.

I decided to study the role of *Ter94* modulation on aggregate density at a few earlier time points namely day 5 and day 10 as well as day 15. I used the pan neuronal *Elav Gal4* to overexpress and knockdown *Ter94* using a *UAS-Ter94* construct and a *UAS-Ter94 RNAi* respectively. I also studied the function of two *Ter94* mutants i.e. *Ter94*^{R152H} and *Ter94*^{A229E}. *Ter94*^{R152H} is a dominant active form of the protein and *Ter94*^{A229E} has been reported to be a null allele. All the fly crosses were incubated at 25 ° C. The F1 progeny was aged for 5, 10 and 15 days before the brains were dissected and stained as per the immunostaining protocol described in materials and methods.

At day 5, there is a slight increase in aggregate density upon modulation of *Ter94* compared to the control (Figure 8). By day 10, the aggregate density starts to decrease in the flies having *Ter94* knocked down as well as overexpressed, overexpression of *Ter94*^{R152H} seems to cause an increase in aggregate density by day 10 (Figure 9). On day 15, we see a significant increase in aggregate density upon overexpression of *Ter94*^{R152H}. Knockdown of *Ter94* and overexpression of *Ter94*^{WT} shows a decrease in aggregate density. Overexpression of *Ter94*^{A229E} does not show any change in aggregate density compared to the respective control groups at any of the 3 time points.

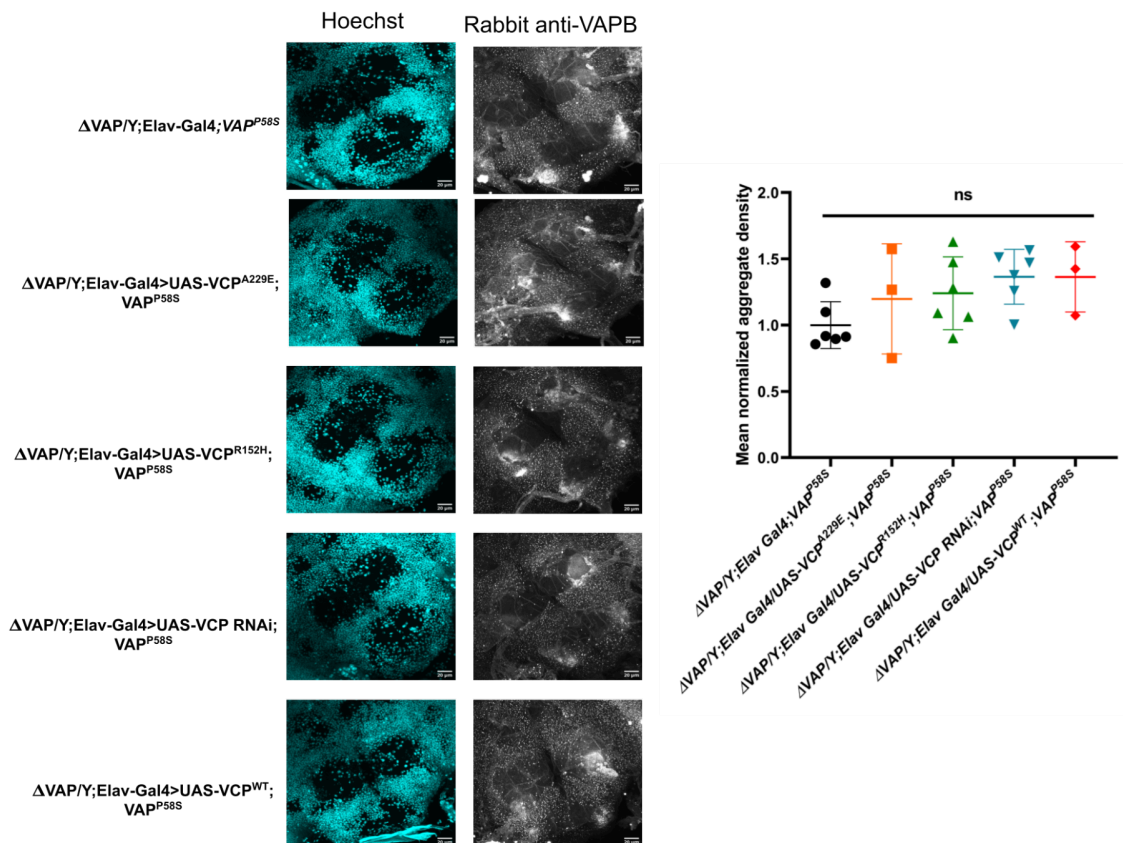


Figure 8: Effect of Ter94 modulation on VAP^{P58S} aggregate density at day 5

At day 5, we see a mild increase in aggregate density upon both overexpression of *Ter94* as well as its RNAi knockdown and also the expression of two mutant forms of *Ter94* i.e. *Ter94*^{R152H} and *Ter94*^{A229E} show some increase in aggregate density. Scale bar: 20 μ m, n = 5, N = 3-5. p value > 0.05; One way ANOVA with Bonferroni correction. The images represent maximum intensity projections.

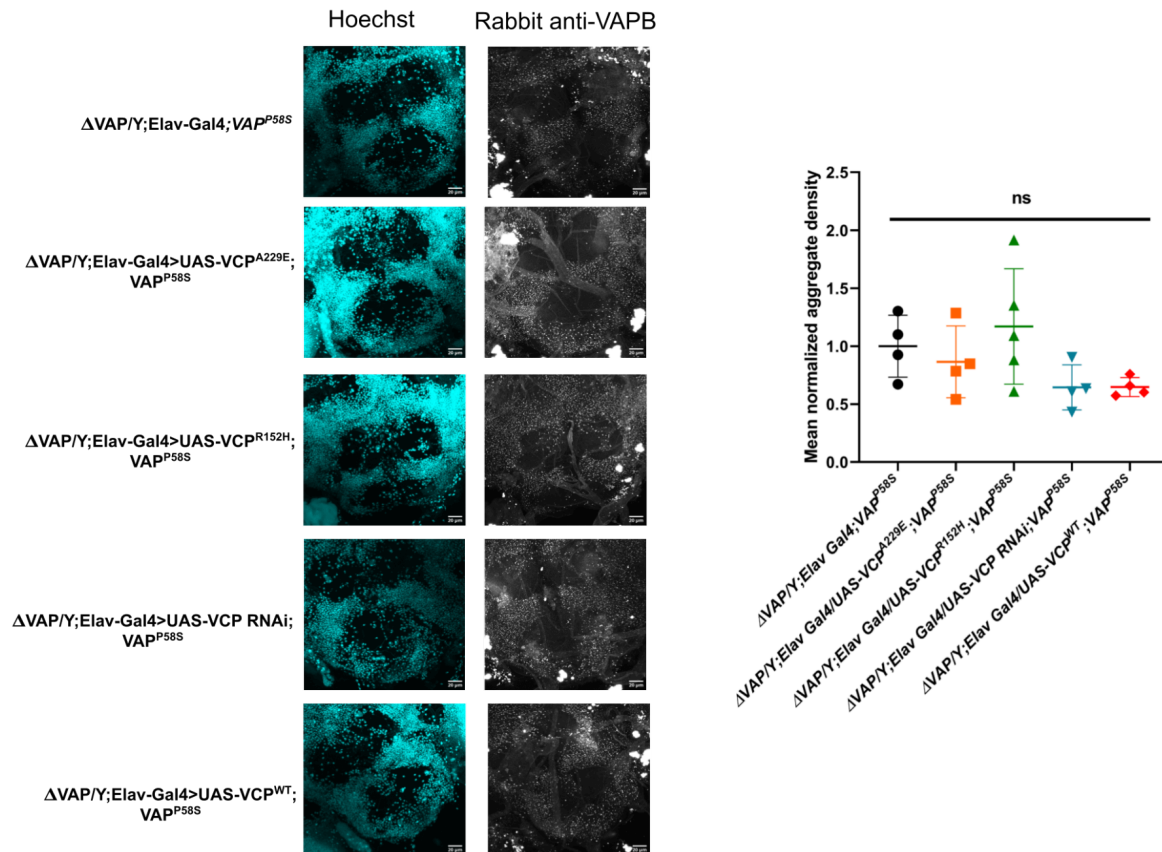


Figure 9: Effect of Ter94 modulation on VAP^{P58S} aggregate density at day 10

On day 10, we see a reduction in aggregate density upon knockdown of *Ter94*. Overexpression of *Ter94* also shows a decrease in aggregate density which is opposite to what we see at day 5. Overexpression of *Ter94*^{R152H} shows a continued increase in aggregate density and overexpression of *Ter94*^{A229E} does not show any change with respect to the control group. Scale bar: 20 μ m, n = 5, N = 4-5. p value > 0.05; One way ANOVA with Bonferroni correction. The images represent maximum intensity projections.

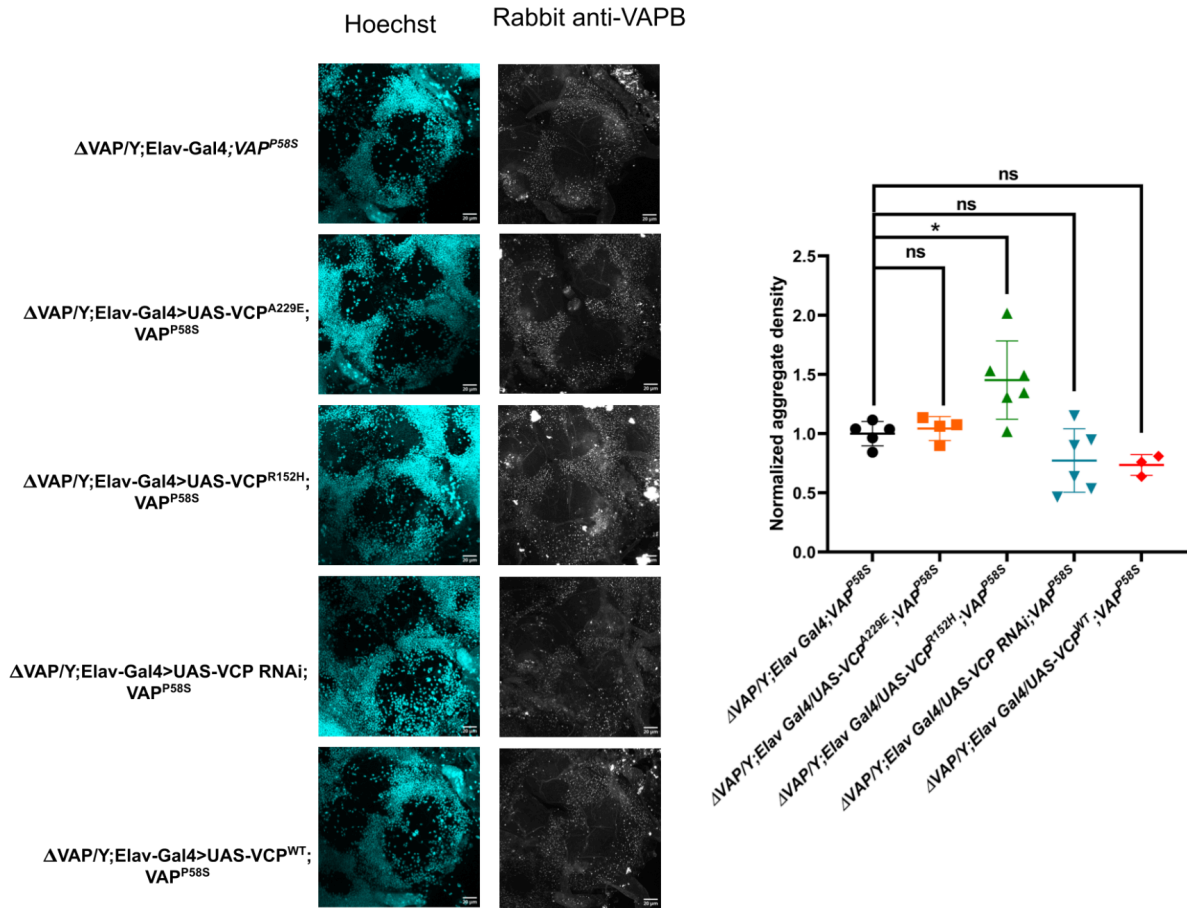


Figure 10: Effect of Ter94 modulation on VAP^{P58S} aggregate density at day 15

On day 15, we see a continued decrease in aggregate density upon *Ter94* knockdown and overexpression as well. Overexpression of *Ter94*^{R152H} also continues to show an increase in aggregate density and overexpression of *Ter94*^{A229E} does not show any difference compared to the control group. Scale bar: 20 μm , n = 5, N = 4-5, *: p < 0.05; One way ANOVA with Bonferroni correction. The images represent maximum intensity projections.

Age dependent change in aggregate density upon *Atg1* modulation

Atg1 is one of the early initiators of autophagy. *Thulasidharan et. al. 2024* have shown that knockdown of *Atg1* causes an increase in aggregate density at day 15 in adult female flies. This suggests that autophagy might have some role to play in aggregate clearance in adult brains.

I knocked down and overexpressed *Atg1* and studied its effect on aggregate density in adult males. I used the pan-neuronal *Elav-Gal4* to drive the overexpression or knockdown. We aged the flies at 25 °C for 5 and 10 days before imaging.

On day 5 we see a slight reduction in aggregate density upon *Atg1* knockdown and *Atg1* overexpression does not show any change in aggregate density (Figure 11). By day 10, the knockdown of *Atg1* seems to show a mild increase in aggregate density compared to its respective control group while *Atg1* overexpression does not seem to change the aggregate density at all (Figure 12). The increase of aggregate density upon *Atg1* knockdown is in line with the data previously reported (*Thulasidharan et. al. 2024*).

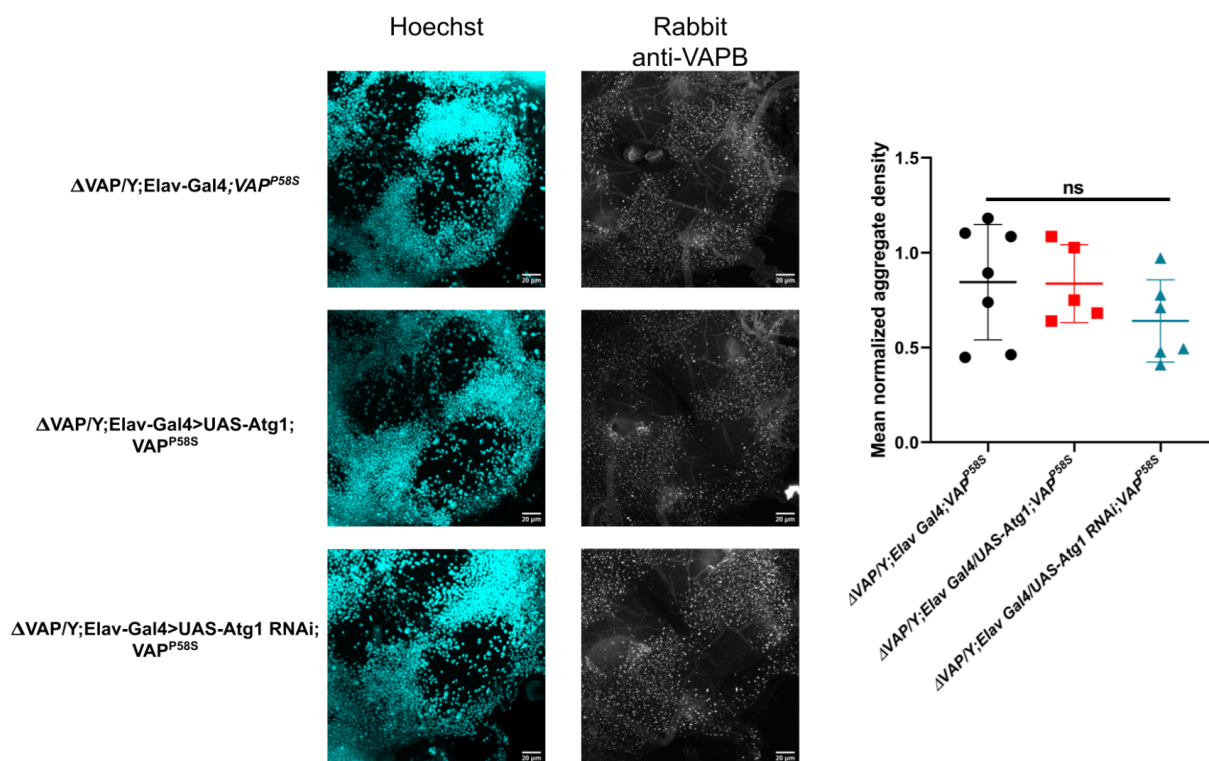


Figure 11: Effect of *Atg1* modulation on aggregate density at day 5 in adult males.

On day 5, we see a slight decrease in aggregate density upon *Atg1* knockdown which is opposite to what we would expect. Overexpression does not show any change in aggregate density. Scale bars 20 μm . $n = 5$; $N = 5-6$; p value > 0.05 ; One way ANOVA with Bonferroni corrections. The images represent maximum intensity projections.

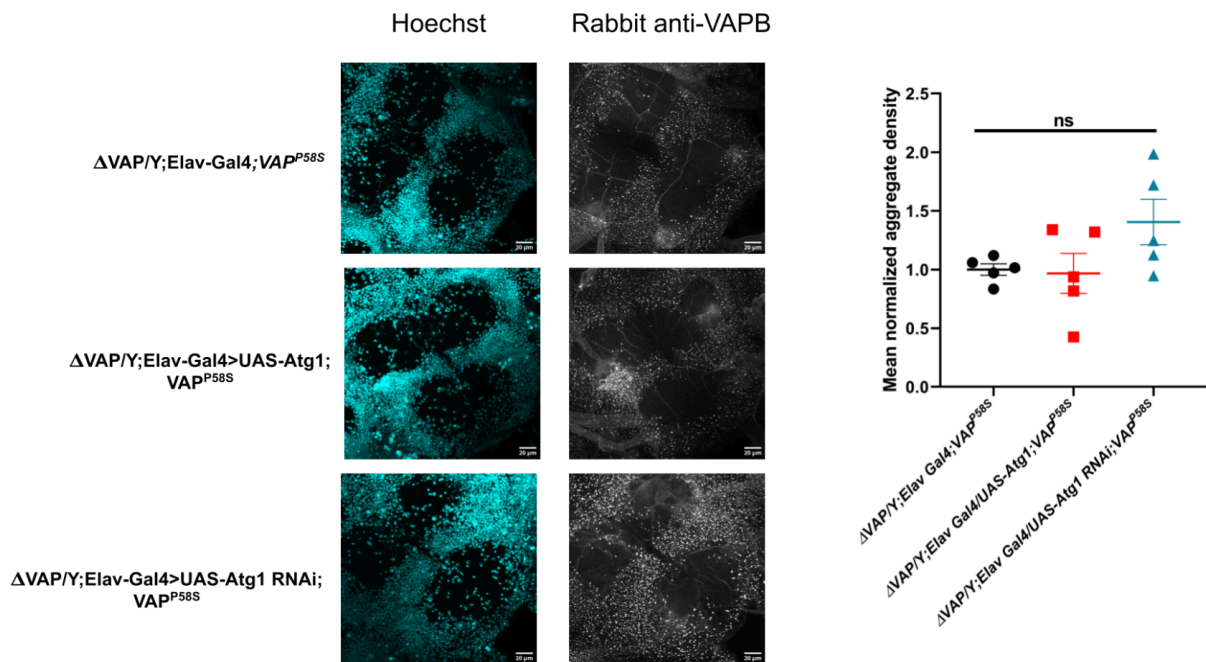


Figure 12: Effect of Atg1 modulation on aggregate density on adult brains at day 10.

On day 10, we do see an increase in aggregate density upon *Atg1* knockdown which is similar to what is expected and what was also shown by *Thulasidharan et. al.* in their study of adult female flies at day 15. Overexpression of *Atg1* however does not show any significant change in aggregate density. Scale bars: 20 μm . n = 5; N = 5-6; p value > 0.05. One way ANOVA with Bonferroni corrections. The images represent maximum intensity projections.

I next wanted to study if the change in aggregate density is also coupled with a change in the motor ability of flies. I overexpressed and knocked down *Atg1* in adult females using a pan-neuronal *Elav-Gal4* and studied their motor activity using a negative geotaxis assay as described in materials and methods.

The female flies have a wild type copy of *VAP* present on the X chromosome which causes rescue of the motor phenotype associated with *VAP*^{P58S}. We see that the control group does not show any motor defects throughout the time of the assay. Knockdown of *Atg1* shows a decrease in motor activity which progressively declines as the fly ages. The *Atg1* overexpression group does not show any decline in motor activity as compared to the control group (Figure 13).

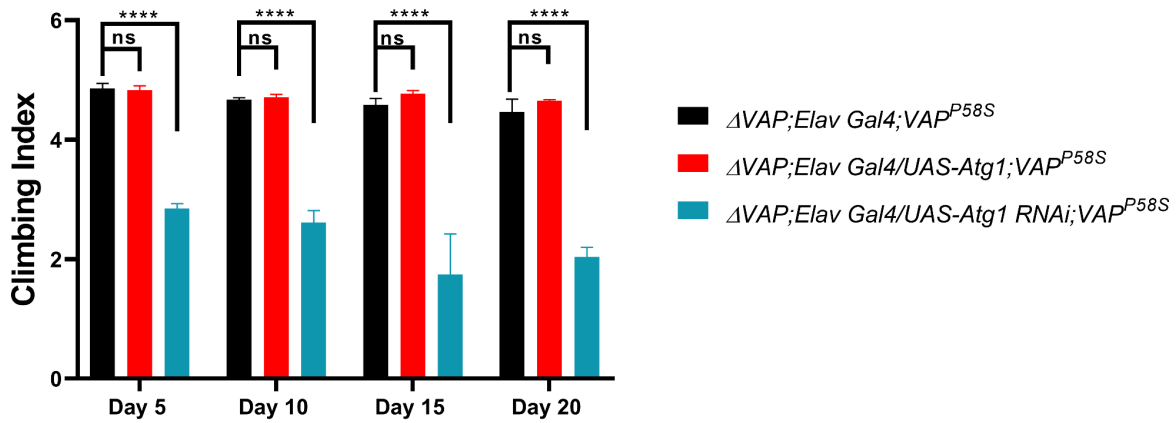


Figure 13: Climbing assay to evaluate the change in motor ability of the flies upon *Atg1* modulation.

The motor assay was performed with female flies of each of the respective genotypes for 20 days post pupal eclosion. *Atg1* knockdown shows a significant decrease in motor activity which progressively gets worse as the fly ages showing a correlation between increase in aggregate density and the motor ability of the fly. *Atg1* overexpression does not make a significant change in activity compared to the control group. $n = 25-30$, $N = 3$; ****: $p < 0.0001$. Two way ANOVA with Dunnett's multiple comparisons.

Age dependent change in aggregate density upon *TOR* modulation in adult males

TOR pathway controls autophagic initiation by binding to the *Ulk1-FIP200* complex in mice. It primarily acts as an inhibitor of autophagy and is also involved in nutrient sensing in the local cellular environment. *mTOR* has also been picked up as a genetic interactor of *VAPB* in previous studies in the lab (*Deivasigamani et. al., 2014*). *mTOR* being an upstream inhibitor of autophagy prompted us to study its role in aggregate modulation in neurons.

I decided to increase the activity of the protein by knocking down one of the upstream inhibitors of the *mTOR* complex. *Tsc1* inhibits raptor which is an activator of the *mTOR* complex. By knocking down the *Tsc1* protein, we tried to prevent the inhibition of raptor and consequently of the *mTOR* complex itself. Presence of a more active *mTOR* complex would then cause further inhibition of the autophagy pathway which should increase the aggregate density as per our hypothesis. We performed the knockdown using *Elav-Gal4* at 25 °C and the F1 progeny was aged for 5 and 15 days before dissections and imaging of brain samples.

We do see an increase in aggregate density upon *Tsc1* knockdown at day 5 conforming to our hypothesis of autophagy being involved in aggregate clearance (Figure 14). However the increase in aggregate density is mitigated by day 15 and aggregate density is similar to the respective control at day 15 (Figure 15).

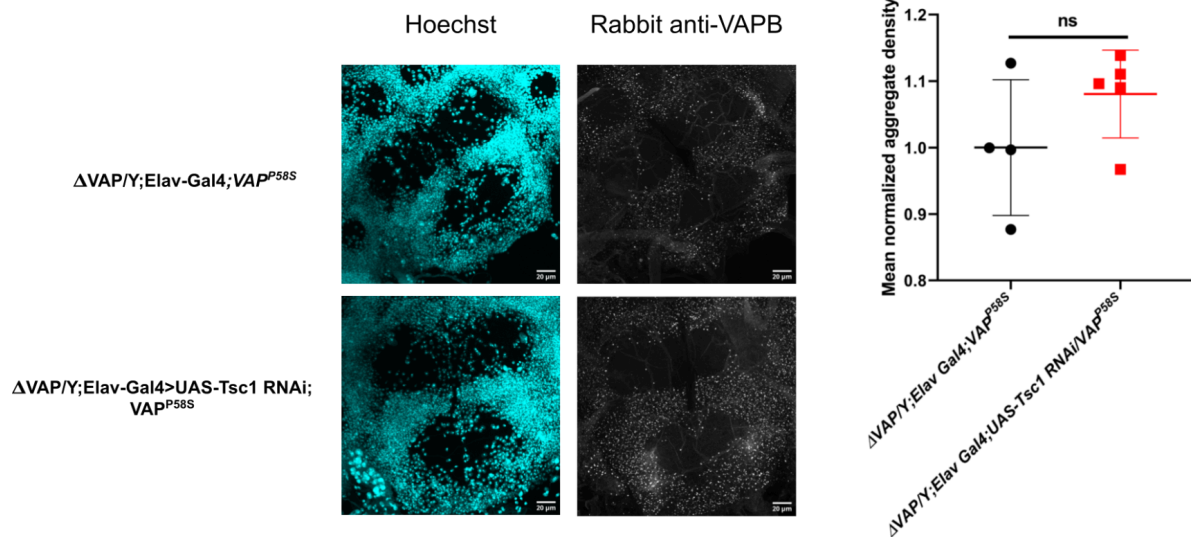


Figure 14: Change in aggregate density upon TOR modulation at day 5 in adult males

Tsc1 is an upstream inhibitor of TOR and knockdown of *Tsc1* would cause an increase in TOR activity of TOR and thus a reduction in autophagic activity in the cell. Knockdown of *Tsc1* seems to cause a slight increase in aggregate density at day 5 compared to the control group. Scale bars: 20 μ m. n = 5, N = 4-5; p value > 0.05. Non parametric T test. The images represent maximum intensity projections.

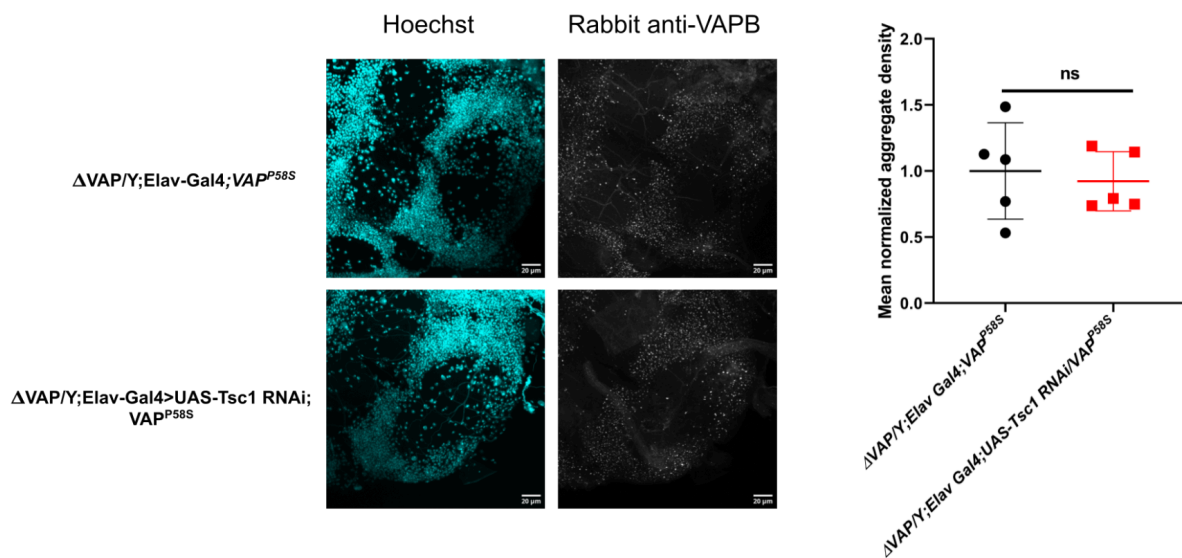


Figure 15: Change in aggregate density upon mTOR modulation at day 15 in adult males.

At day 10, there is no significant change in aggregate density upon *Tsc1* knockdown as compared to the control group. Scale bars: 20 μ m; n = 5, N = 5; p value > 0.05. Non parametric T test. The images represent maximum intensity projections.

Chapter 4: Discussion and Future Perspectives

VAPB has been known to be associated with ER stress and its P58S mutation has been used extensively in the lab to model ALS-like phenotypes in flies. VAPB^{P58S} flies show a reduced lifespan and impaired motor activity (*Thulasidharan A. et. al., 2024*). These flies also show presence of VAP positive aggregates in both the larval and adult brains and the aggregate density is dependent on the dose of the mutant protein. Introduction of VAP^{WT} clears these aggregates in an age dependent manner, however the clearance mechanism is not very well understood.

The study done by *Thulasidharan et. al. 2024* explored autophagy and proteasomal pathways (through Ter94) as clearance pathways for VAPB aggregates in adult fly brains. They showed that autophagy is actively involved in clearing aggregates in the adult brain but the role of Ter94 seems to be complex and not straightforward. They had also explored the role of Reactive Oxygen Species (ROS) mediated clearance through SOD1 but it didn't seem to be active in adults. The major gap that remained was how does the aggregate density change in an age dependent manner in adult fly brains. The work done so far in the thesis tries to address this question and shed some light on the age dependent dynamics of aggregate clearance.

According to the paper, knockdown of *Ter94* causes a reduction in aggregates at day 15 and I do see a similar trend upon *Ter94* knockdown as the fly ages from day 5 to day 15. However it is not statistically significant. On day 15, it was shown that overexpression of Ter94^{R15H} shows a significant increase in aggregate density and when the overexpression is studied in an age dependent manner, it seems to agree with the observation albeit with a lower significance. The paper also talks about an increase in aggregate density upon Ter94 overexpression at day 15, however, the current data does not seem to agree with this trend. Ter94^{WT} overexpression causes a slight increase in aggregate density at day 5 but by day 10 and day 15, the density reduces compared to their respective controls. Ter94^{R152H} is reported as a dominant active form of the protein and the deviation in trends for Ter94^{R152H} and Ter94^{WT} is intriguing. Ter94^{A229E} is a loss of function allele for *ter94* and its overexpression in the fly does not seem to be bringing any change in aggregate density as the fly ages. The data presented in this thesis supplements the work done by *Thulasidharan et. al.* and gives a stronger foundation to further investigate the role of the protein in aggregate clearance.

The role of autophagy was explored using *Atg1* knockdown in the paper. Knockdown of *Atg1* showed a significant increase in aggregate density at day 15 in female flies. The data suggests an important role played by autophagy as the female fly already has a wild type copy of VAP at the X chromosome and VAP^{WT} is already known to reduce aggregate density. The increase in aggregate density because of *Atg1* knockdown seems to suggest that VAP^{WT} and *Atg1* are working together to clear aggregates. I wanted to study this interaction hence it was important to study the effect of *Atg1* knockdown in male flies which do not have a wild type copy of VAPB. *Atg1* knockdown is lethal in flies so because of the reduction in progeny numbers, I could only study the aggregate density at day 5 and day 10 and I do see a similar trend in aggregate density as described in the paper. It does increase at day 10 however the increase is not as significant as described in the paper. I also studied *Atg1* overexpression to further supplement the data and the aggregate density was similar to control for both day 5 and day 10. These results seem to suggest that VAP^{WT} does seem to be working with *Atg1* to clear the aggregates. The molecular change in aggregate density in females upon *Atg1* knockdown has also been supplemented by a motor assay to check for the climbing ability of flies. The data shows a reduction in climbing ability in female flies upon *Atg1* knockdown in an age dependent manner. Overexpression of *Atg1* does not show a significant change. There is a clear correlation between aggregate density and motor ability of flies however any causal relationships could not be established. All of these data combined point to a possible interaction between VAP^{WT} and *Atg1* to clear aggregates. It is also reported that *Atg1* contains an FFAT motif which is a canonical motif recognized by VAP (*Zhao et. al. 2018*). This further supports the hypothesis that both of these proteins are interacting with each other. Further study of this interaction would be able to shed more light on a possible mechanism of aggregate clearance.

One of the upstream protein regulation autophagy is TOR protein (*Noda et. al. 1998*). It binds to the ULK1, FIP200 and *Atg13* and keeps it from activating. In order to activate autophagy, TOR dissociates from the complex and the complex then gets phosphorylated to further activate downstream steps of autophagy (*Hosokawa et. al. 2009*). TOR has also been picked up as a genetic interactor of VAP in one of the studies previously done in the lab (*Deivasigamani et. al., 2014*). It is this relationship between TOR, autophagy and VAP that motivated the study of the effect of TOR modulation on aggregate density. *Tsc1* is an upstream inhibitor of TOR and we used its knockdown as a proxy for increasing activity of TOR in the cell. The increased activity of tor should further inhibit autophagy and that is indeed what we saw, however the effect was not long lasting and we see a reversion of aggregation density to control levels by day 15. This result further supports the idea that

autophagy is indeed active in adult brains and is actively working to clear the protein aggregates.

The work done so far uncovers some of the role played by autophagy as a major player in clearance of VAP^{P58S} aggregates in an age dependent manner in the adult fly brain. Many open questions still remain to be answered. For instance the interaction between Atg1 and VAP through the FFAT motif in the protein is an interesting aspect to be studied further. Literature indicates that there is an interaction between Atg1 and VAP in cell lines (*Zhao et. al. 2018*), between VAP and Ter94 in flies (*Tendulkar et. al., 2022*) and interaction between Atg1 and VCP in mice (*Wang et. al., 2019*). It would be interesting to study this three way interaction between these proteins to uncover more details about aggregate dynamics in the fly brain and ultimately about the progression of ALS.

References

1. Bose, J.K., Huang, C.C., and Shen, C.K.J. (2011). Regulation of autophagy by neuropathological protein TDP-43. *Journal of Biological Chemistry* 286, 44441-44448.
2. Chaplot K., Pimpale L., Ramalingam B., Deivasigamani S., Kamat S., Ratnaparkhi G., (2019). SOD1 activity threshold and TOR signalling modulate VAP(P58S) aggregation via reactive oxygen species-induced proteasomal degradation in a *Drosophila* model of amyotrophic lateral sclerosis. *Disease models and mechanisms*. 12.
3. Chua J., Calbiac D. H., Kabashi E., Bamada S., (2022). Autophagy and ALS: mechanistic insights and therapeutic implications. *Autophagy* 18:2, 254-282.
4. Chu, S., Xie, X., Payan, C., and Stochaj, U. (2023). Valosin containing protein (VCP): initiator, modifier, and potential drug target for neurodegenerative diseases. *Molecular Neurodegeneration* 18, 52-52.
5. Cozzi, M., and Ferrari, V. (2022). Autophagy Dysfunction in ALS: from Transport to Protein Degradation. *Journal of Molecular Neuroscience* 72, 1456-1481.
6. Deivasigamani, S., Verma, H.K., Ueda, R., Ratnaparkhi, A., and Ratnaparkhi, G.S. (2014). A genetic screen identifies Tor as an interactor of VAPB in a *Drosophila* model of amyotrophic lateral sclerosis. *Biology open* 3, 1127-1138.
7. Feldman, E.L., Goutman, S.A., Petri, S., Mazzini, L., Savelieff, M.G., Shaw, P.J., and Sobue, G. (2022). Amyotrophic lateral sclerosis. *Lancet (London, England)* 400, 1363-1363.
8. Ferrari, V., Cristofani, R., Tedesco, B., Crippa, V., Chierichetti, M., Casarotto, E., Cozzi, M., Mina, F., Piccolella, M., Galbiati, M., *et al.* (2022). Valosin Containing Protein (VCP): A Multistep Regulator of Autophagy. *International journal of molecular sciences* 23, 1939-1939.
9. Gal, J., Ström, A.L., Kilty, R., Zhang, F., and Zhu, H. (2007). p62 Accumulates and Enhances Aggregate Formation in Model Systems of Familial Amyotrophic Lateral Sclerosis. *Journal of Biological Chemistry* 282, 11068-11077.
10. Gal, J., Ström, A.L., Kwinter, D.M., Kilty, R., Zhang, J., Shi, P., Fu, W., Wooten, M.W., and Zhu, H. (2009). Sequestosome 1/p62 links familial ALS mutant SOD1 to LC3 via an ubiquitin-independent mechanism. *Journal of neurochemistry* 111, 1062-1073.

11. Gurney, M.E., Pu, H., Chiu, A.Y., Dal Canto, M.C., Polchow, C.Y., Alexander, D.D., Caliendo, J., Hentati, A., Kwon, Y.W., Deng, H.X., *et al.* (1994). Motor neuron degeneration in mice that express a human Cu,Zn superoxide dismutase mutation. *Science (New York, N.Y.)* *264*, 1772-1775.
12. Hill, S.M., Wrobel, L., Ashkenazi, A., Fernandez-Estevez, M., Tan, K., Bürli, R.W., and Rubinsztein, D.C. (2021). VCP/p97 regulates Beclin-1-dependent autophagy initiation. *Nature Chemical Biology* *2021 17:4 17*, 448-455.
13. Hosokawa, N., Hara, T., Kaizuka, T., Kishi, C., Takamura, A., Miura, Y., Iemura, S.I., Natsume, T., Takehana, K., Yamada, N., *et al.* (2009). Nutrient-dependent mTORC1 Association with the ULK1–Atg13–FIP200 Complex Required for Autophagy. *Molecular biology of the cell* *20*, 1981-1981.
14. Ju, J.S., Fuentealba, R.A., Miller, S.E., Jackson, E., Piwnica-Worms, D., Baloh, R.H., and Weihl, C.C. (2009). Valosin-containing protein (VCP) is required for autophagy and is disrupted in VCP disease. *Journal of Cell Biology* *187*, 875-888.
15. Kang, R., Zeh, H.J., Lotze, M.T., and Tang, D. (2011). The Beclin 1 network regulates autophagy and apoptosis. In *Cell death and differentiation*, pp. 571-580.
16. Klickstein, J.A., Johnson, M.A., Antonoudiou, P., Maguire, J., Paulo, J.A., Gygi, S.P., Weihl, C., and Raman, M. (2024). ALS-related p97 R155H mutation disrupts lysophagy in iPSC-derived motor neurons. *Stem Cell Reports* *19*, 366-382.
17. Larroquette, F., Seto, L., Gaub, P.L., Kamal, B., Wallis, D., Larivière, R., Vallée, J., Robitaille, R., and Tsuda, H. (2015). Vapb/Amyotrophic lateral sclerosis 8 knock-in mice display slowly progressive motor behavior defects accompanying ER stress and autophagic response. *Human molecular genetics* *24*, 6515-6515.
18. Lev, S., Halevy, D. ben, Peretti, D., and Dahan, N. (2008). The VAP protein family: from cellular functions to motor neuron disease. *Trends in Cell Biology* *18(6)*, 282–290.
19. Liu, W., Zhu, S.o., Guo, Y.l., Tu, L.f., Zhen, Y.q., Zhao, R.y., Ou-Yang, L., Kurihara, H., He, R.R., and Liu, B. (2023). BL-918, a small-molecule activator of ULK1, induces cytoprotective autophagy for amyotrophic lateral sclerosis therapy. *Acta Pharmacologica Sinica* *44*, 524-537.
20. Mejzini R., Flynn L., Pitout I., Fletcher S., Wilton S., Akkari P., (2019) ALS Genetics, Mechanisms and Therapeutics: Where are We Now?. *Frontiers in Neuroscience* *13*, 1310.

21. Moustaqim-barrette, A., Lin, Y.Q., Pradhan, S., Neely, G.G., Bellen, H.J., and Tsuda, H. (2013). The amyotrophic lateral sclerosis 8 protein, VAP, is required for ER protein quality control. *Human molecular genetics* 23, 1975-1975.
22. Nguren D., Thombre R., Wang J., (2019). Autophagy as a Common Pathway in Amyotrophic Lateral Sclerosis. *Neuroscience letters* 697, 34-48.
23. Nishimura, A.L., Mitne-Neto, M., Silva, H.C.A., Richieri-Costa, A., Middleton, S., Cascio, D., Kok, F., Oliveira, J.R.M., Gillingwater, T., Webb, J., *et al.* (2004). A Mutation in the Vesicle-Trafficking Protein VAPB Causes Late-Onset Spinal Muscular Atrophy and Amyotrophic Lateral Sclerosis. *American journal of human genetics* 75, 822-822.
24. Noda, T., and Ohsumi, Y. (1998). Tor, a Phosphatidylinositol Kinase Homologue, Controls Autophagy in Yeast. *Journal of Biological Chemistry* 273, 3963-3966.
25. Osaka, M., Ito, D., and Suzuki, N. (2016). Disturbance of proteasomal and autophagic protein degradation pathways by amyotrophic lateral sclerosis-linked mutations in ubiquilin 2. *Biochemical and biophysical research communications* 472, 324-331.
26. Parzych, K.R., and Klionsky, D.J. (2014). An Overview of Autophagy: Morphology, Mechanism, and Regulation. *Antioxidants & Redox Signaling* 20, 460-460.
27. Pontifex, C.S., Zaman, M., Fanganiello, R.D., Shutt, T.E., and Pfeffer, G. (2024). Valosin-Containing Protein (VCP): A Review of Its Diverse Molecular Functions and Clinical Phenotypes. *International journal of molecular sciences* 25.
28. Rosen, D.R., Siddiquet, T., Patterson, D., Figlewicz, D.A., Sapp, P., Hentatit, A., Donaldson, D., Goto, J., O, J.P., Dengt, H.-X., *et al.* (1993). Mutations in Cu/Zn superoxide dismutase gene are associated with familial amyotrophic lateral sclerosis.
29. Şentürk, M., Lin, G., Zuo, Z., Mao, D., Watson, E., Mikos, A.G., and Bellen, H.J. (2019). Ubiquilins regulate autophagic flux through mTOR signalling and lysosomal acidification. *Nature cell biology* 21, 384-396.
30. Tendulkar, S., Hegde, S., Garg, L., Thulasidharan, A., Kaduskar, B., Ratnaparkhi, A., and Ratnaparkhi, G.S. (2022). Caspar, an adapter for VAPB and TER94, modulates the progression of ALS8 by regulating IMD/NFκB-mediated glial inflammation in a *Drosophila* model of human disease. *Human molecular genetics* 31, 2857-2875.
31. Thulasidharan, A., Garg, L., Tendulkar, S., and Ratnaparkhi, G.S. (2024). Age-dependent dynamics of neuronal VAPBALS inclusions in the adult brain. *Neurobiology of Disease* 196.
32. Tresse, E., Salomons, F.A., Vesa, J., Bott, L.C., Kimonis, V., Yao, T.P., Dantuma, N.P., and Taylor, J.P. (2010). VCP/p97 is essential for maturation of ubiquitin-containing

- autophagosomes and this function is impaired by mutations that cause IBMPFD. *Autophagy* 6, 217-217.
33. Tripathi, P., Guo, H., Dreser, A., Yamoah, A., Sechi, A., Jesse, C.M., Katona, I., Doukas, P., Nikolin, S., Ernst, S., *et al.* (2021). Pathomechanisms of ALS8: altered autophagy and defective RNA binding protein (RBP) homeostasis due to the VAPB P56S mutation. *Cell death & disease* 12, 466-466.
 34. Wang, B., Maxwell, B.A., Joo, J.H., Gwon, Y., Messing, J., Mishra, A., Shaw, T.I., Ward, A.L., Quan, H., Sakurada, S.M., *et al.* (2019). ULK1 and ULK2 Regulate Stress Granule Disassembly Through Phosphorylation and Activation of VCP/p97. *Molecular cell* 74, 742-757.e748.
 35. Wu, D., Hao, Z., Ren, H., and Wang, G. (2018). Loss of VAPB Regulates Autophagy in a Beclin 1-Dependent Manner. *Neuroscience bulletin* 34, 1037-1037.
 36. Xia, D., Tang, W.K., and Ye, Y. (2016). STRUCTURE AND FUNCTION OF THE AAA+ ATPASE p97/Cdc48p. *Gene* 583, 64-64.
 37. Xia, Q., Wang, H., Hao, Z., Fu, C., Hu, Q., Gao, F., Ren, H., Chen, D., Han, J., Ying, Z., *et al.* (2016). TDP -43 loss of function increases TFEB activity and blocks autophagosome–lysosome fusion. *The EMBO journal* 35, 121-142.
 38. Zhao, Y.G., Liu, N., Miao, G., Chen, Y., Zhao, H., and Zhang, H. (2018). The ER Contact Proteins VAPA/B Interact with Multiple Autophagy Proteins to Modulate Autophagosome Biogenesis. *Current biology : CB* 28, 1234-1245.e1234.